



## Accepted Article

**Title:** Universal Electrochemical Synthesis of Mesoporous Chalcogenide Semiconductors: Mesoporous CdSe and CdTe Thin Films for Optoelectronic Applications

**Authors:** Tomota Nagaura, Hoang-Phuong Phan, Victor Malgras, Tuan-Anh Pham, Hyunsoo Lim, Aditya Ashok, Jeonghun Kim, Jungmok You, Nam-Trung Nguyen, Jongbeom Na, and Yusuke Yamauchi

This manuscript has been accepted after peer review and appears as an Accepted Article online prior to editing, proofing, and formal publication of the final Version of Record (VoR). This work is currently citable by using the Digital Object Identifier (DOI) given below. The VoR will be published online in Early View as soon as possible and may be different to this Accepted Article as a result of editing. Readers should obtain the VoR from the journal website shown below when it is published to ensure accuracy of information. The authors are responsible for the content of this Accepted Article.

**To be cited as:** *Angew. Chem. Int. Ed.* 10.1002/anie.202013541

**Link to VoR:** <https://doi.org/10.1002/anie.202013541>

## RESEARCH ARTICLE

# Universal Electrochemical Synthesis of Mesoporous Chalcogenide Semiconductors: Mesoporous CdSe and CdTe Thin Films for Optoelectronic Applications

Tomota Nagaura,<sup>[a]+</sup> Hoang-Phuong Phan,<sup>[b]+</sup> Victor Malgras,<sup>[c]</sup> Tuan-Anh Pham,<sup>[b]</sup> Hyunsoo Lim,<sup>[a]</sup> Aditya Ashok,<sup>[a]</sup> Jeonghun Kim,<sup>[d]</sup> Jungmok You,<sup>[e]</sup> Nam-Trung Nguyen,<sup>[b]</sup> Jongbeom Na\*<sup>[a]</sup> and Yusuke Yamauchi\*<sup>[a,c]</sup>

- [a] T. Nagaura, H. Lim, A. Ashok, Dr. J. Na, Prof. Y. Yamauchi  
Australian Institute for Bioengineering and Nanotechnology (AIBN) and School of Chemical Engineering, The University of Queensland, Brisbane, Queensland 4072, Australia  
E-mail: [j.na@uq.edu.au](mailto:j.na@uq.edu.au); [y.yamauchi@uq.edu.au](mailto:y.yamauchi@uq.edu.au)
- [b] Dr. H.-P. Phan, T.-A. Pham, Prof. N.-T. Nguyen  
Queensland Micro- and Nanotechnology Centre, Griffith University, Brisbane, 4111 Queensland, Australia
- [c] Dr. V. Malgras, Dr. Jongbeom Na, Prof. Y. Yamauchi  
JST-ERATO Yamauchi Material Space-Tectonics, International Center for Materials Nanoarchitectonics (WPI-MANA) and International Center for Young Scientists (ICYS), National Institute for Materials Science (NIMS), 1-1 Namiki, Tsukuba, Ibaraki 305-0044, Japan
- [d] Prof. J. Kim  
Department of Chemistry, Kookmin University, Seoul 02707, Republic of Korea
- [e] Prof. J. You  
Department of Plant and Environmental New Resources, Kyung Hee University, 1732 Deogyong-daero, Giheung-gu, Yongin-si, Gyeonggi-do 446-701, Republic of Korea
- + These authors equally contributed to this work

Supporting information for this article is given via a link at the end of the document.

**Abstract:** Here we report the soft-template-assisted electrochemical deposition of mesoporous semiconductors (CdSe and CdTe). The resulting mesoporous films are stoichiometrically equivalent and contain mesopores homogeneously distributed over the entire surface. To demonstrate the versatility of the method, two block copolymers with different molecular weights are used, yielding films with pores of either 9 or 18 nm diameter. As a proof of concept, the mesoporous CdSe film based photodetectors show a high sensitivity of  $204 \text{ mW}^{-1} \text{ cm}^2$  at 680 nm wavelength, which is at least two orders of magnitude more sensitive than the bulk counterpart. This work pioneers a new synthesis route for nanostructured semiconductors with optical band gaps active in the visible spectrum.

## Introduction

Engineering the architecture of nanomaterials, namely nanoarchitectonics, has been a hot spot of research with the aim to understand and elaborate strategies towards designing and functionalizing semiconductors at the supra-atomic/molecular level. The last decade has seen remarkable advancement and rapid growth in broad varieties of nanoarchitected platforms, including quantum dots,<sup>[1-2]</sup> nanowires,<sup>[3-4]</sup> nanotubes,<sup>[5]</sup> and nanorods.<sup>[6-7]</sup> A great deal of fundamental researches has been successfully transitioned into commercial products such as solar cells and light emitting diodes that employ quantum dots.<sup>[8-9]</sup> In these practical applications, group II-VI semiconductors, such as CdX, ZnX, PbX, etc. (X = chalcogenide), have demonstrated the best performance due to their optical properties and stability. At the nanoscale, controlling the morphological aspects, such as the particle size, can have a direct impact on the electronic or optical

properties.<sup>[10-11]</sup> For example, the narrow emission band of room- or low-temperature quantum dot-laser, now commonly used in optical commutation devices or various medical applications, can be tuned directly through their size.<sup>[12]</sup> Such quantum dots-lasers have been already commercialized using III-V semiconductors. Core-shell nanoarchitecture comprising II-VI semiconductors also shows distinctive optical properties, such as the conversion of visible light into infrared, which can be applied to photovoltaic or photoconductive devices.<sup>[13]</sup> Heterostructured CdSe/CdS nanoparticles were shown to be more efficient than CdSe for the photocatalytic generation of hydrogen.<sup>[14]</sup> Recently, carbon nitride also has attracted a great interest due to its outstanding optical performance, such as photoluminescence (PL) and electrochemiluminescence.<sup>[15-16]</sup> Especially, its nanosheets distinctively enhance PL performance.<sup>[17]</sup> Thus, several types of recently developed nanoarchitectures have demonstrated superior performance in a wide range of applications. Among numerous types of nanoarchitectures, mesoporous semiconductors have emerged as a new class of materials that can enable light reflection/scattering inside the nanoporous structures, thus attracting a great deal of interest for optical sensors and solar cells. In addition, II-VI semiconducting mesopores can be down-scaled below the electron mean free path, leading to interesting physical phenomena such as quantum confinement and surface scattering.<sup>[18-19]</sup> These features expectedly open-up the pathway to understand and to engineer optoelectronic systems with unexplored capabilities.

Mesoporous materials with different compositions can be prepared through self-assembly process, providing a versatile platform for a wide range of applications, including solar cells with large-interface p-n junctions,<sup>[20-21]</sup> photoelectrochemical cells,<sup>[22-23]</sup> and biosensors.<sup>[24]</sup> Until now, semiconducting CdX (X=Te, Se, S,

## RESEARCH ARTICLE

etc.) nanoparticles have been successfully embedded in mesoporous matrix to benefit from a maximum surface area.<sup>[25]</sup> Quantum dots of II-VI semiconductors, such as CdTe and CdSe, have been prepared by an electrochemical method,<sup>[26]</sup> and those composite films with other materials, *i.e.* mesoporous silica,<sup>[27]</sup> enable to produce quantum dot arrays. However, a CdX mesoporous structure with regular and monodisperse porosity have rarely been reported. Although there have been reports of CdX reverse opal structure fabricated by infiltrating the semiconducting nanocrystals inside the cavities between sacrificial colloidal crystals,<sup>[28]</sup> reducing the pore size to the mesoscale enables drastically high surface area. In addition, the several steps involved in the hard-templating approach, including preparation of the template, precursor filling, and template removal, makes the procedure tedious and inflexible. While soft-templates made of lyotropic liquid crystal (LLC) seem an appropriate option to consider,<sup>[29-30]</sup> their high viscosity forbid their use at larger scales, and pore sizes are limited to less than 10 nm, due to the small molecular weights.

To tackle these challenges, the present study introduces an innovative and simple electrochemical approach to synthesize mesoporous CdSe and CdTe films in the presence of stable polystyrene-*b*-poly(ethylene oxide) (PS-*b*-PEO) block copolymer micelles (Figure 1). This method provides significant control over the pore size (ranging from 5 to 50 nm) and density while ensuring excellent uniformity.<sup>[31-34]</sup> The elimination of complex steps, costly materials, and sophisticated CVD processes makes our method a ubiquitous approach, suitable for low cost and mass production of mesoporous CdX semiconductors. This soft-template method has been widely applied to synthesize mesoporous metals and metal oxides,<sup>[35]</sup> but the possible compositions have been limited so far. Chalcogenide semiconductors enable to design narrower energy bandgap in comparison with metal oxide semiconductors. It is indispensable to optimize the chalcogenide nanostructures for controlling chemical and physical properties. To demonstrate potential applications, we develop optical sensors using the as-synthesized mesoporous CdSe films. The as-fabricated devices exhibit excellent characteristics for optoelectronic applications, where the use of the mesoporous architectures can significantly enhance the photosensitivity. Our unique but simple electrochemical technique can be considered a game-changing technology for mesoporous semiconductors-based devices, bringing exciting opportunities to both the academic and industrial research community.

## Results and Discussion

Figure 1 shows a schematic illustration of the mesoporous CdX films, while the detailed experimental setup can be found in the supporting information (Figures S1-3 and Tables S1-2). The average size of micelles formed from PS(5,000)-*b*-PEO(2,000) is calculated to be around 12.0 nm with 15 % coefficient of validation, according to our transmission electron microscopy (TEM) study (Figure S4). The stability and sturdiness of these micelles are ideal to template the synthesis of mesoporous materials. From the field emission scanning electron microscopy (FE-SEM) analysis, the mesoporous films appear smooth and densely populated with mesopores (Figures 2a-b, 2d-e). Samples prepared with the PS(5,000)-*b*-PEO(2,000) and PS(10,000)-*b*-PEO(4,100) are decorated with pores of 9.0-9.5 nm and 17.7-18.0 nm,

respectively, regardless of their chalcogenide composition (Figure 2g). The pore sizes are dependent on the molecular weight of the block copolymer as the pores are created by PS cores. Each coefficient of validation is also within the comparable range as 19-25 %. On the other hand, reference CdX samples deposited without block copolymers do not contain any porosity (Figures 2c, f).

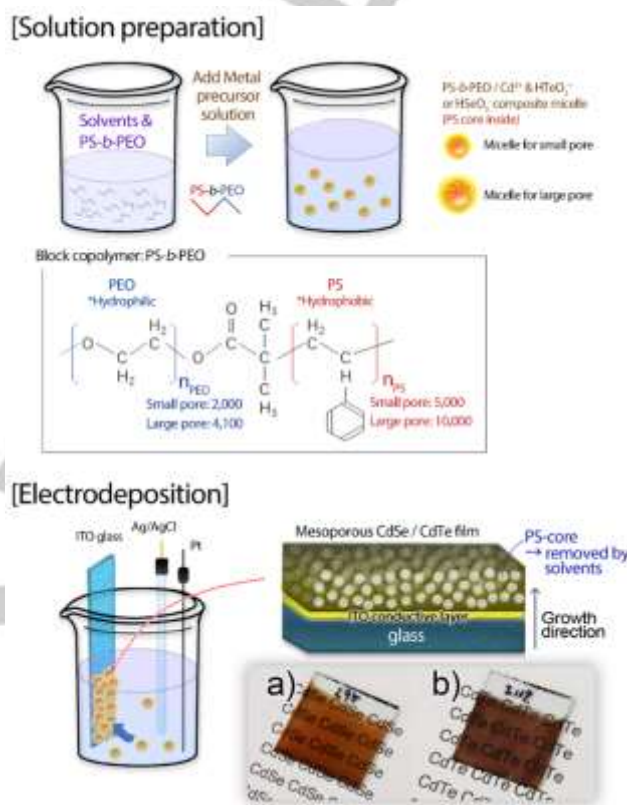


**Figure 1.** Schematic illustrating the fabrication and morphologic structure of the mesoporous CdX films, along with photographs of the as-deposited (a) CdSe and (b) CdTe films, grown on ITO glass.

Following the thickness evolution investigation, we observe a linear dependence on the supplied charge ( $Q$ ) (Figure S5). The growth rate of the CdSe and CdTe films are  $5.8 \times 10^{-5} \text{ cm}^3 \text{ C}^{-1}$  and  $4.4 \times 10^{-5} \text{ cm}^3 \text{ C}^{-1}$ , respectively. Although the ion valance of both Te and Se in solution is expected to be 4, the electrodeposition of CdSe films is more efficient. This synthesis method can be applied to any conductive substrates, *i.e.* conductive oxides or metallic substrates. Figure S6 shows SEM images show that films grown on Au substrates have similar mesoporous structures.

The film surface was further evaluated by X-ray photoelectron spectroscopy (XPS), resolved on Cd 3d, Se 3d, and Te 3d (Figure S7). Each peak was identified by XPS referential data.<sup>[36]</sup> The Cd 3d doublet appears at almost the same positions. In addition to the expected  $3d_{5/2}$  chalcogenide peaks in CdSe and CdTe, located at 53.9 and 572.0 eV, the species observed at 58.9 and 575.9 eV can be assigned to surface oxidation, such as  $\text{SeO}_2$  and  $\text{TeO}_2$ , respectively. While the oxide contribution appears minor for CdSe, it is dominant in the CdTe film. The XRD patterns of the CdSe and CdTe films are shown in Figures 3a-b. Previous report demonstrated that electrodeposited CdSe film can form a hexagonal and/or cubic structure, depending on the applied

## RESEARCH ARTICLE

synthetic condition.<sup>[37-38]</sup> In our mesoporous CdSe film, the XRD patterns can be assigned to a hexagonal/cubic mixture (ICDD PDF 00-008-459 and 00-029-0292, respectively). From the strongest (002) peak, the crystallite sizes of all the films are calculated to be 7.8 to 9.7 nm using the Scherrer equation. The CdTe films show a cubic structure (ICDD PDF 00-015-0770), with crystallite sizes of 8.7-11.0 nm, calculated from the (111) peak. Both EDS and XPS analyses also confirmed a one-to-one stoichiometry for each CdX sample (Figure S8). This proves that each element is well distributed throughout the pore walls, and not segregated in a core-shell configuration.

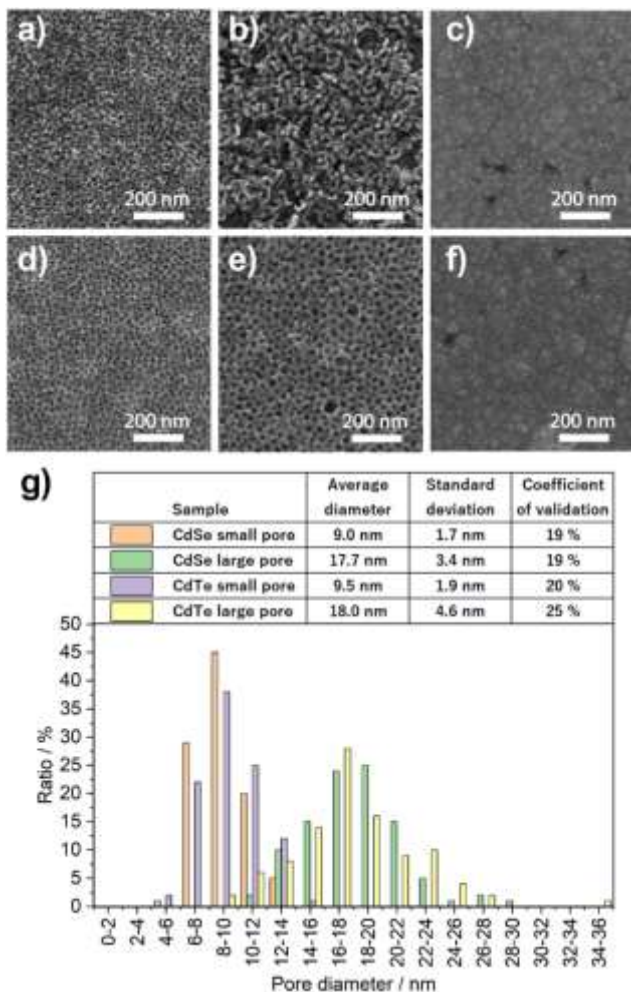


**Figure 2.** Top-view FE-SEM images of the CdSe (a-c) and CdTe (d-f) films prepared (a,d) with PS(5,000)-*b*-PEO(2,000), (b,e) with PS(10,000)-*b*-PEO(4,100), (c,f) without block copolymers. (g) Pore size distribution calculated from each SEM image.

Our previous study has demonstrated that the addition of these solvents, such as tetrahydrofuran (THF), gives significant effects on pore size expansion due to micelle swelling.<sup>[39]</sup> The solvents used in this study to dissolve the block copolymers, *N,N*-dimethylformamide (DMF), and THF, are expected to have a strong influence on the resulting nanostructure. The effect of THF content on the morphology was investigated on mesoporous CdTe with large pores prepared with PS(10,000)-*b*-PEO(4,100) (Figure S9). Below a certain threshold, micelles have a higher probability to merge or agglomerate, yielding a disordered

morphology along with the presence of spherical particles on the surface. It is indicated that an appropriate amount of THF plays a role to produce flat film surface in the micrometer scale. On the other hand, with excessive THF, larger defects and/or island start to appear due to a more diluted micellar solution. Only under optimal conditions can the deposition produce uniformly sized mesopores.

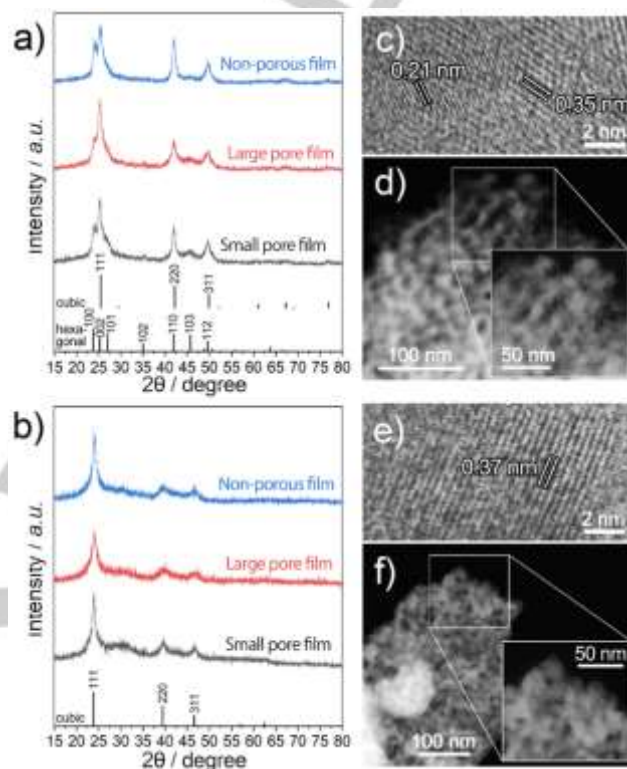


**Figure 3.** XRD patterns from the (a) CdSe and (b) CdTe films (with small and large pores as well as non-porous reference). HR-TEM images with lattice fringes (c,e) and HAADF-STEM images (d,f) of the CdSe (c,d) and CdTe films (e,f).

The high-angle annular dark-field imaging (HAADF-STEM) images show that both mesoporous CdSe and CdTe films prepared with PS(5,000)-*b*-PEO(2,000) are decorated with 9 nm pores (Figures 3d,f), while the walls are made of grains of similar size. On the high-resolution transmission electron microscopy (HR-TEM) images, the lattice distances of the CdSe film can either be assigned to the (002) and (110) planes of hexagonal or the (111) and (220) planes of cubic structure (Figure 3c). The fringes measured for the CdTe film can be assigned to the (111) plane of a cubic structure (Figure 3e). These results are in good agreement with the XRD data. The EDS mapping in Figure S10 confirms that each element is homogeneously dispersed in the structure in a one-to-one stoichiometry.

This study is the first example of mesoporous CdSe and CdTe semiconducting films fabricated through an electrochemical soft-templating approach. Such a mesoporous architecture offers several superior properties over non-porous films, including high surface area, which is suitable for various applications such as electrochemical sensing, drug delivery, and optoelectronic devices. As proof of concepts for potential applications, we assembled highly sensitive photodetectors using the as-

## RESEARCH ARTICLE

synthesized mesoporous CdSe film as photo-absorber. All the synthesized CdSe films have 1.71-1.72 eV band gap energy calculated by Tauc plot on UV-visible absorption spectroscopy (Figure S11), as could be expected from hexagonal and cubic CdSe.<sup>[40-41]</sup> The illustration in Figure 4a presents the successive steps necessary to fabricate the sensor, consisting of a 300 nm-thick aluminum layer deposited on top of the CdSe film (Figure S12). A standard lithography process was then applied to shape the micro-electrodes, followed by the wet-etching of the aluminum (using  $\text{H}_3\text{PO}_4 + \text{HNO}_3 + \text{CH}_3\text{COOH}$ ). It should be noted that CdSe reacts with  $\text{HNO}_3$ .<sup>[42]</sup> Hence, the ITO/CdSe Schottky junction can be well-confined under the Al electrode area with a cross sectional area of  $200 \mu\text{m}$  in diameter (Figure S13). The device was then mounted onto a PCB board for wire-bonding (Figure 4b), and optical illumination with a wavelength of  $\lambda=680 \text{ nm}$  was applied to investigate the light-response of the as-fabricated sensors (Figure S14).

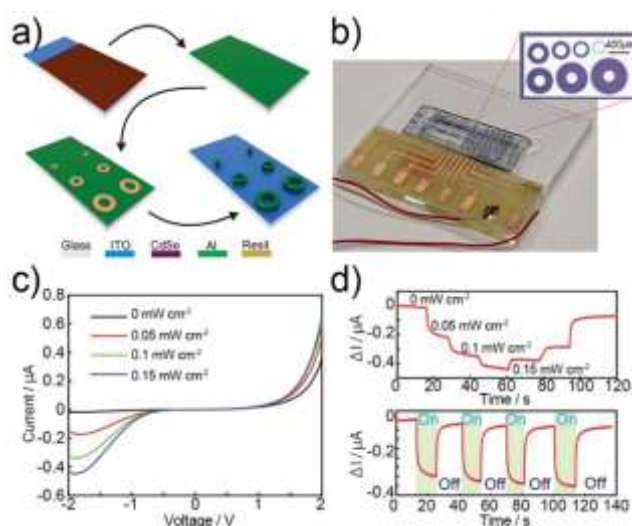


**Figure 4.** Demonstration of optical sensors using mesoporous CdSe films. (a) Fabrication process; (b) Photograph of the fabricated device; (c) I-V response of the mesoporous CdSe samples (small pores); (d) The change in the current of the mesoporous samples under variation of illumination intensity (top), and constant intensity of  $0.1 \text{ mW cm}^{-2}$  (bottom).

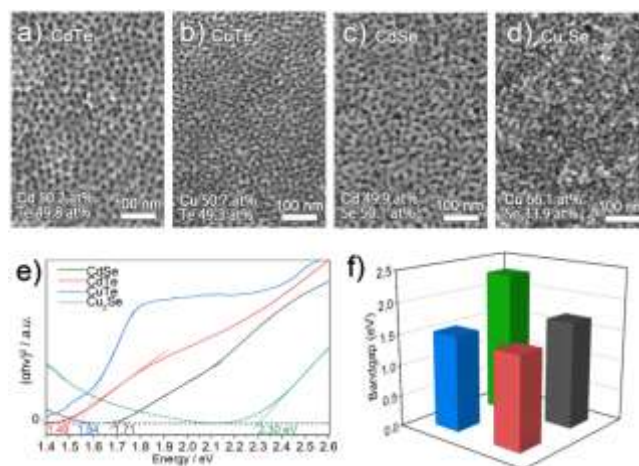
For a comprehensive comparison of the optical properties of the CdSe film-based devices, we also developed photodetectors from non-porous CdSe film. Figure S15 shows the I-V response of the CdSe films without pores (150 nm in thickness) under light intensities varying from 0 to  $0.15 \text{ mW cm}^{-2}$ , and a relatively small photocurrent was detected. The photo-to-dark current ratio (PDCR) is found to be 0.059 at a light intensity of  $0.05 \text{ mW cm}^{-2}$ , yielding an optical sensitivity (S) of  $1.18 \text{ mW}^{-1} \text{ cm}^2$  (details on calculations can be found in the supplementary information). It is also worth noting that the I-V curve of the sensors exhibits a back-to-back diode behavior due to the Schottky barriers between ITO/CdSe (0.77 eV) as well as between CdSe/Al (0.5 eV).<sup>[42]</sup>

Figure 4c presents the response of the photodetectors fabricated with the mesoporous CdSe film (ca. 9 nm in pore size and 150 nm in film thickness). Evidently, a much more significant change in the current is observed when the sensors are subjected to illumination. The PDCR of the mesoporous CdSe structures-based sensors is found to be 10 at  $0.05 \text{ mW cm}^{-2}$ , corresponding to a sensitivity of  $S = 204 \text{ mW}^{-1} \text{ cm}^2$ . This result indicates that

mesoporous architecture obviously enhances the sensitivity of the optical sensors and achieves quite competitive performance among reported chalcogenide films (Table S3). This excellent sensitivity combined with the simple fabrication process are promising aspects to promote electrochemically synthesized CdX towards high performance optoelectronics (Table S3).

We hypothesized that the remarkable improvements in the light-sensitivity of the optical sensors was attributed to (i) the low dark current and (ii) the efficiency of light trapping in the mesoporous CdSe structure. As evidenced by Figure 4c, the dark current of the mesoporous CdSe device is much lower than that of the non-porous samples. The mesoporous architecture consists of numerous electrical semiconducting junctions as observed in TEM data of the CdSe pores (Figure S16), which are typically longer than the nonporous films, as illustrated in Figure S17a.<sup>[43]</sup> In addition, the size of grains and pores with ca. 9 nm is smaller than the mean free path of electrons of n-type CdSe ( $\sim 20 \text{ nm}$ ),<sup>[44]</sup> and can contribute to increase the resistivity under dark conditions.<sup>[18-19]</sup> These phenomena would result in a smaller dark current, which in turn leads to a higher PDCR (i.e., reversely proportional to  $I_{\text{dark}}$ ). Moreover, the nano-junctions formed in the mesoporous structure can be directly exposed to the light as light can penetrate and scatter through the nanopore networks (Figure S17b). This phenomenon could play an important role in the enhancement of the quantum efficiency of the sensors.<sup>[45]</sup>

The repeatability of the mesoporous CdSe-based sensors was then investigated by measuring the response of the current at a fixed applied voltage of  $-1.5 \text{ V}$  over time (I-t curve in Figure 4d). The current increases and decreases incrementally and synchronically with the light intensity, and the sensor shows a consistent current change over several light illumination cycles (Figure 4d). It should also be pointed out that there is a time delay in the response of the sensors, which has been commonly observed among various semiconductor-based photodetectors.<sup>[46]</sup> A typical phenomenon causing the time decay is the trapped charges (e.g. surface/interface charges, crystal defects) in the semiconductor films. The time decay can be minimized by employing a built-in micro heater, to release the trapped charges through thermal activations.<sup>[47]</sup>



**Figure 5.** Surface SEM images and EDS analysis on mesoporous films of (a) CuTe, (b) CdTe, (c) CdSe, and (d)  $\text{Cu}_2\text{Se}$ . (e) Tauc-plot on UV-Visible spectroscopy and (f) bandgap of CuTe (blue), CdTe (red), CdSe (black), and  $\text{Cu}_2\text{Se}$  (green).

## RESEARCH ARTICLE

This report aims to explore a new route to fabricate mesoporous semiconductors through single-step electrochemical synthesis. The homogeneous internal mesopores have been successfully well-formed in the synthesized mesoporous CdSe and CdTe films. These results show the high potential and availability for synthesizing other semiconductors by using this single-step method. Thus, four different types of semiconductors (CuTe, CdTe, CdSe, and Cu<sub>2</sub>Se) are prepared, analyzed, and investigated to demonstrate the applicability, as shown in Figure 5. The stoichiometric compositions and the energy bandgap of each semiconductor film were analyzed and determined through EDS, UV-Vis spectroscopy results, and Tauc plot. Those chemical binding energies were further characterized by XPS (Figure S18). The Te peaks on CuTe reveals the comparable tendency to CdTe film in Figure S7d, and the Cu peaks also show Cu (II) signals with its satellite peaks, suggesting the surface has been oxidized, same as CdTe and CdSe systems. In contrast, the Cu<sub>2</sub>Se have a little oxidation peak, indicating it has resistivity against the surface oxidation. Although the single-step soft template methods using block copolymers have generally been applied to metals or metal oxides in the synthesis of porous materials, it also shows applicability to porous semiconductor materials, according to Figure 5. As the porous CdSe photodetector indicates, it can expect very high applicability of various mesoporous semiconductor materials. Furthermore, the energy bandgap can be controlled according to each semiconductor combination and composition, which is expected to be applicable to semiconductor material applications widely.

## Conclusion

We have reported a novel route for mesoporous semiconductor (CdSe and CdTe) synthesis by employing a simple electrochemical process. 3D mesoporous architecture would attribute to high sensitivity in optical sensor using 680 nm wavelength laser. In addition, the single-step synthesis method can be applied to various semiconductors, and the energy band gap can be tuned through the composition and combination of semiconductor materials. As a result, the suggested synthesis method of mesoporous semiconductor films shows a high possibility for various applications, as well as visible or near-infrared sensors.

## Acknowledgements

The authors acknowledge the financial support from JX Nippon Mining & Metals Corporation. This research was supported by Basic Science Research Program through the National Research Foundation of Korea (NRF) funded by the Ministry of Education (2020R1A6A3A03039037). This work was also performed in part at the Queensland node of the Australian National Fabrication Facility (ANFF-Q), a company established under the National Collaborative Research Infrastructure Strategy to provide nano and microfabrication facilities for Australian researchers.

**Keywords:** mesoporous semiconductors • self-assembly • electrochemical deposition • block copolymers

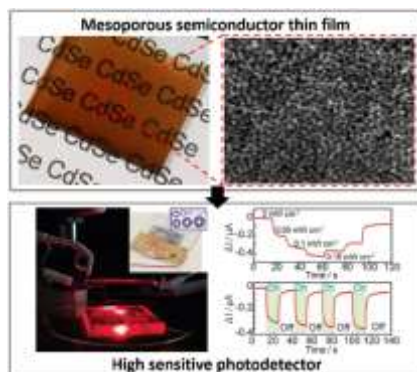
- [1] C. B. Murray, D. J. Norris, M. G. Bawendi, *J. Am. Chem. Soc.* **1993**, *115*, 8706-8715.
- [2] V. L. Colvin M. C. Schlamp, A. P. Alivisatos, *Nature* **1994**, *370*, 354-357.
- [3] H. Yu, J. Li, R. A. Loomis, P. C. Gibbons, L. W. Wang, W. E. Buhro, *J. Am. Chem. Soc.* **2003**, *125*, 16168-16169.
- [4] J. W. Sun, L. W. Wang, W. E. Buhro, *J. Am. Chem. Soc.* **2008**, *130*, 7997-8005.
- [5] X. Jiang, B. Mayers, T. Herricks, Y. Xia, *Adv. Mater.* **2003**, *15*, 1740-1743.
- [6] X. Peng, L. Manna, W. Yang, J. Wickham, E. Scher, A. Kadavanich, A. P. Alivisatos, *Nature* **2000**, *404*, 59-61.
- [7] Z. A. Peng, X. Peng, *J. Am. Chem. Soc.* **2001**, *123*, 183-184.
- [8] H. Chen, C. Hsu, H. Hong, *IEEE Photonics Technol. Lett.* **2006**, *18*, 193-195.
- [9] A. P. Alivisatos, *Science* **1996**, *271*, 933-937.
- [10] M. Bruchez, M. Moronne, P. Gin, S. Weiss, A. P. Alivisatos, *Science* **1998**, *281*, 2013-2016.
- [11] M. Han, X. Gao, J. Z. Su, S. Nie, *Nat. Biotechnol.* **2001**, *19*, 631-635.
- [12] V. I. Klimov, A. A. Mikhailovsky, S. Xu, A. Malko, J. A. Hollingsworth, C. A. Leatherdale, H.-J. Eisler, M. G. Bawendi, *Science* **2000**, *290*, 314-317.
- [13] S. Kim, B. Fisher, H.-J. Eisler, M. Bawendi, *J. Am. Chem. Soc.* **2003**, *125*, 11466-11467.
- [14] F. Qiu, Z. Han, J. J. Peterson, M. Y. Odoi, K. L. Sowers, T. D. Krauss, *Nano Lett.* **2016**, *16*, 5347-5352.
- [15] G. Peng, L. Xing, J. Barrio, M. Volokh, M. Shalom, *Angew. Chem. Int. Ed.* **2018**, *57*, 1186-1192.
- [16] D. Han, D. Ni, Q. Zhou, J. Ji, Y. Lv, Y. Shen, S. Liu, Y. Zhang, *Adv. Funct. Mater.* **2019**, *29*, 1905576.
- [17] T. Zhao, Q. Zhou, Y. Lv, D. Han, K. Wu, L. Zhao, Y. Shen, S. Liu, Y. Zhang, *Angew. Chem. Int. Ed.* **2020**, *59*, 1139-1143.
- [18] E. H. Sondheimer, *Adv. Phys.* **1952**, Vol. 1.
- [19] Z. Liu, P. C. Searson, *J. Phys. Chem. B* **2006**, *110*, 4318-4322.
- [20] W. A. Badawy, *J. Adv. Res.* **2015**, *6*, 123-132.
- [21] K. A. Salman, Z. Hassan, K. Omar, *Int. J. Electrochem. Sci.* **2012**, *7*, 376-386.
- [22] B. O'Regan, M. Grätzel, *Nature* **1991**, *353*, 737-740.
- [23] F. Cao, G. Oskam, G. J. Meyer, P. C. Searson, *J. Phys. Chem.* **1996**, *100*, 17021-17027.
- [24] A. Jane, R. Dronov, A. Hodges, N. H. Voelcker, *Trends Biotechnol.* **2009**, *27*, 230-239.
- [25] P. Wang, Y. Zhu, X. Yang, C. Li, H. L. Du, *Acta Mater.* **2008**, *56*, 1144-1150.
- [26] Y. Golan, J. L. Hutchison, I. Rubinstein, G. Hodes, *Adv. Mater.* **1996**, *8*, 631-633.
- [27] Y.-T. Kim, J. H. Han, B. H. Hong, Y.-U. Kwon, *Adv. Mater.* **2010**, *22*, 515-518.
- [28] L. Yang, Z. Yang, W. Cao, L. Chen, J. Xu, H. Zhang, *J. Phys. Chem. B* **2005**, *109*, 11501-11504.
- [29] I. S. Nandhakumar, T. Gabriel, X. Li, G. S. Attard, M. Markham, D. C. Smith, J. J. Baumberg, *Chem. Commun.* **2004**, 1374-1375.
- [30] X. Li, I. S. Nandhakumar, T. Gabriel, G. S. Attard, M. L. Markham, D. C. Smith, J. J. Baumberg, K. Govender, P. O'Brien, D. Smyth-Boyle, *J. Mater. Chem.* **2006**, *16*, 3207-3214.
- [31] H. Wang, L. Wang, T. Sato, Y. Sakamoto, S. Tominaka, K. Miyasaka, N. Miyamoto, Y. Nemoto, O. Terasaki, Y. Yamauchi, *Chem. Mater.* **2012**, *24*, 1591-1598.
- [32] C. Li, Ö Dag, T. D. Dao, T. Nagao, Y. Sakamoto, T. Kimura, O. Terasaki, Y. Yamauchi, *Nat. Commun.* **2015**, *6*, 6608.
- [33] M. Iqbal, Y. V. Kaneti, K. Kashimura, M. Yoshino, B. Jiang, C. Li, B. Yuliarto, Y. Bando, Y. Sugahara, Y. Yamauchi, *Nanoscale Horiz.* **2019**, *4*, 960-968.
- [34] D. Baba, J. Kim, J. Henzie, C. Li, B. Jiang, Ö Dag, Y. Yamauchi, T. Asahi, *Chem. Commun.* **2018**, *54*, 10347-10350.
- [35] H. Lim, K. Kani, J. Henzie, T. Nagaura, A. S. Nugraha, M. Iqbal, Y. S. Ok, M. S. A. Hossain, Y. Bando, K. C. W. Wu, H.-J. Kim, A. E. Rowan, J. Na, Y. Yamauchi, *Nat. Protoc.* **2020**, *15*, 2980-3008.
- [36] J. F. Moulder, W. F. Stickle, P. E. Sobol, K. D. Bomben, *Handbook of X-ray Photoelectron Spectroscopy*, ed J. Chastain (Perkin-Elmer Corp.), **1992**.

## RESEARCH ARTICLE

- [37] S. M. Pawar, A. V. Moholkar, C. H. Bhosale, *Mater. Lett.* **2007**, *61*, 1034-1038.
- [38] S. M. Rashwan, S. M. Abd El-Wahab, M. M. Mohamed, *J. Mater. Sci.: Mater. Electron.* **2007**, *18*, 575-585.
- [39] C. Li, M. Iqbal, J. Lin, X. Luo, B. Jiang, V. Malgras, K. C.-W. Wu, J. Kim, Y. Yamauchi, *Acc. Chem. Res.* **2018**, *51*, 1764-1773.
- [40] B. G. Streetman, S. Banerjee, *Solid State electronic Devices*, 5th ed. New Jersey, **2000**.
- [41] S. Ninomiya, S. Adachi, *J. Appl. Phys.* **1995**, *78*, 4681-4689.
- [42] H. Suzuki, *Jpn. J. Appl. Phys.* **1966**, *5*, 1253-1254.
- [43] J. Cai, W. Wei, X. Hu, D. A. Wood, *Earth-Sci. Rev.* **2017**, *171*, 419-433.
- [44] M. C. Beard, G. M. Turner, C. A. Schmuttenmaer, *Nano Lett.*, **2002**, *2*, 983-987.
- [45] Y. Qiu, W. Liu, W. Chen, W. Chen, G. Zhou, P.-C. Hsu, R. Zhang, Z. Liang, S. Fan, Y. Zhang, Y. Cui, *Sci. Adv.* **2016**, *2*, e1501764.
- [46] J. Reemts, A. Kittel, *J. Appl. Phys.* **2007**, *101*, 013709.
- [47] M. Hou, H. So, A. J. Suria, A. S. Yalamathy, D. G. Senesky, *IEEE Electron Device Lett.* **2016**, *38*, 56-59.

## RESEARCH ARTICLE

## Entry for the Table of Contents



The concept of this work demonstrates a novel route for film synthesis of mesoporous semiconductors and its application. The pore size can be controlled by the molecular weight of the block copolymers and the synthesized mesoporous CdSe film exhibits a high sensitivity of  $204 \text{ mW}^{-1} \text{ cm}^2$  on 680 nm as a photodetector. This method suggests the facile synthesis process and shows a high potential for new optoelectronic applications.